A Simultaneous Design and Optimization Framework for the Reaction and Distillation Sections of Methanol to Olefins Process

Authors:

Ning Li, Liwen Zhao, Dan Li, Huifeng Sun, Di Zhang, Guilian Liu

Abstract:

The reaction and separation sections are the keys to the methanol-to-olefins (MTO) chemical processes, and they should be optimized to reduce the cost of production. This work develops a framework for the simultaneous design and optimization of the reaction and distillation sections. An optimization model with shortcut and rigorous methods combined is established for distillation columns to improve accuracy and efficiency. With the auxiliary devices and the selection of utilities considered, the reaction and distillation sections are integrated to maximize profits. The genetic algorithm targets the optimal parameters, including the catalyst's coke content and reaction temperature, each column's operating pressure, and the allocation of utilities and auxiliary devices. For the studied MTO process, the optimal reaction temperature and catalyst's coke content were identified to be 496 °C and 7.8%, respectively. The maximum profit is 15.3% greater than that identified with only the separation section optimized, and the minimum total annual cost (TAC) of the separation section is 3.73% less.

Article

A Simultaneous Design and Optimization Framework for the Reaction and Distillation Sections of Methanol to Olefins Process

Ning Li [1], Liwen Zhao [1], Dan Li [1], Huifeng Sun [1], Di Zhang [2],* and Guilian Liu [1],*

1   School of Chemical Engineering and Technology, Xi'an Jiaotong University, Xi'an 710049, China
2   Inner Mongolia Electric Power Survey & Design Institute Co., Ltd., Hohhot 010011, China
*   Correspondence: zhangdi9860@126.com (D.Z.); guilianliui@mail.xjtu.edu.cn (G.L.)

Abstract: The reaction and separation sections are the keys to the methanol-to-olefins (MTO) chemical processes, and they should be optimized to reduce the cost of production. This work develops a framework for the simultaneous design and optimization of the reaction and distillation sections. An optimization model with shortcut and rigorous methods combined is established for distillation columns to improve accuracy and efficiency. With the auxiliary devices and the selection of utilities considered, the reaction and distillation sections are integrated to maximize profits. The genetic algorithm targets the optimal parameters, including the catalyst's coke content and reaction temperature, each column's operating pressure, and the allocation of utilities and auxiliary devices. For the studied MTO process, the optimal reaction temperature and catalyst's coke content were identified to be 496 °C and 7.8%, respectively. The maximum profit is 15.3% greater than that identified with only the separation section optimized, and the minimum total annual cost (TAC) of the separation section is 3.73% less.

Keywords: methanol to olefins; distillation; reaction; model; optimization

1. Introduction

The methanol-to-olefin (MTO) process [1] transfers methanol to ethylene and propylene, and is an important way to produce olefin independently of petroleum. It can help to improve the stable supply of olefin in China [2], as methanol can be derived from coal or natural gas. The MTO reaction was first proposed in the 1970s, with ZSM-5 as the catalyst [3]. Currently, the primary catalyst used in the MTO process is SAPO-34, the total selectivity of ethylene and propylene can reach 80%, and their ratio is adjustable in the interval 0.5~1.5 [4]. Three leading MTO technologies which have been successfully applied in industries [5] are the DMTO developed by Dalian Institute of Chemical Physics (DICP), the SMTO by Sinopec Shanghai Research Institute of Petrochemical Technology, and the MTO technology developed by UOP/Norsk Hydro. The reaction and separation sections are the keys to these processes.

The conversion of methanol and the selectivity to olefin are two key parameters to evaluate the MTO reactor's performance, and are expected to be as high as possible. However, the reactor parameters might have different influences on them. For example, multiple reactions are in progress, and their reaction rates increase along with the reactor's temperature as does the conversion. In comparison, the variation trend of selectivity might differ depending on all reaction rates and their ratios. For the distillation columns of the separation section, lower energy consumption and capital cost are expected while ensuring the purification of olefin products. Many parameters, such as pressure, reflux ratio, and the number of stages, affect these costs. In addition, the utilities selected for condensers and reboilers directly affect the heat exchange areas and energy costs. The costs of heat exchangers, pumps, and compressors arranged between two adjacent columns are related to the neighboring columns' feeds, products, and operating parameters. All of these

columns and auxiliary devices are affected by the separation section's feed and, thus, the reactor parameters. For the optimization of the MTO process, the reaction and separation sections should be considered together with the primary parameters optimized.

For the MTO reactors, the cracking of C_4^+ was promoted in order to increase the production of ethylene and propylene by improving the reactor and optimizing the coke distribution on the catalyst [6]. Moreover, much research on the MTO reaction's mechanism has been carried out [7], including the MTO reactions with the conversions between alkanes and alkenes [8], the kinetic parameters, the relationships between temperature and reaction rates [9], an eight-lumped kinetic model [10] and a seven-lumped kinetic model [11]. The kinetic mechanism models are complex, require much calculation for simulation and optimization, and sometimes cannot converge.

In the separation section, the optimization of distillation is of great significance for energy savings and pollution reductions, and can be achieved based on shortcut and rigorous methods. The Fenske–Underwood–Gilliland (FUG) method is well-known for its simplification and efficiency [12], and is widely applied. Ye et al. [13] extended the Underwood equation to columns with side streams and optimized the distillation sequence considering the condensers and reboilers. Cui [14] established the optimization procedure based on the FUG model and determined the operating pressure according to the minimum annual cost. For the thermally coupled reactive distillation, Gomez-Castro [15] proposed a method to minimize the heat load of columns and illustrated its performance for targeting the optimal design. The boundary value method (BVM) was proposed by Fidkowski [16] to design a distillation column and check the feasibility of the design. Lucia et al. [17] proposed the shortest stripping line approach to target the minimum energy demand. However, shortcut models are usually based on the assumptions of constant molar overflow and constant relative volatilities, which might cause significant errors.

Rigorous models can identify accurate and detailed results for the distillation columns [18]. They are based on material balances (M), equilibrium relationships (E), summation of compositions (S), and enthalpy balances (H), and are known as MESH equations. These equations have been embedded in commercial software, such as Aspen Plus and Unisim, for the design and sensitive analysis of distillation columns [19]. However, distillation sequences with multiple columns can only be designed sequentially, and poor results might be obtained [20].

All columns should be optimized simultaneously, considering their interactions. Viswanathan et al. [21] used the mixed integer nonlinear programming (MINLP) method to optimize a distillation column with the number of theoretical stages as the decision variable. The MESH equations are used in the optimization model as the constraints, and other process parameters are taken as decision variables [22]. The model includes thousands of equations and variables or more, and the challenges are concentrated on the initialization and convergence of the model. In some methods, the MESH equations are pre-solved to establish the mappings among different variables. Seidel et al. [23] proposed an approach for infeasible path optimization of distillation-based flowsheets. Although this method can significantly reduce the number of decision variables, the difficulty lies in establishing an appropriate solution model.

Some research has been carried out for the optimization of the MTO process. Based on Aspen Plus software, Yu [24] simulated the process, proposed an improved design with lower cost, and compared different methods of separating propane and propylene [25]. Dimian [26] studied the heat integration of the MTO process and provided an energy-efficient design. Chen et al. [27] optimized the refrigeration cycle of the MTO process and proposed an alternative arrangement with better economic performance. Although these studies optimized the MTO processes to some extent, the interactions between the reaction and separation sections were left out of consideration.

Different methods and models have been developed to integrate the reaction and separation systems. Yin et al. [28] proposed a method to automatically identify the optimal distillation sequences and generate the appropriate solutions according to different reaction parameters. Hentschel et al. [29] combined the kinetic reaction model with the FUG

model to minimize the total cost of the reaction–distillation process. Both methods can analyze and sort multiple alternative schemes efficiently. Kong et al. [30] proposed an optimization framework for biofuel production based on the superstructure model for synthesizing the process and allocating utilities simultaneously. Based on the generalized model description, critical characteristic identification, and model integration, Ryu et al. [31] proposed a general model for simultaneously optimizing the reaction, separation, and heat exchanger network. Although the MINLP model was generally used to optimize the reaction–separation system [32], it is not easy to solve and target its global optimum. In addition, stochastic optimization algorithms can be used to solve large-scale MINLP problems efficiently, such as genetic algorithm [33], simulated annealing algorithm [34], and particle swarm optimization [35]. Among these, the genetic algorithm is widely used for optimizing complex systems.

Although some researchers have studied the optimization of the MTO process and the integration of the reaction and separation systems, there are no reports about the systematic integration of the reaction and separation sections in the available literature. In the MTO reactor, coke is formed at high temperatures. It attaches to the catalyst's surface and affects its activity, hence the reactor's conversion and selectivity, the separation section, and the energy consumption. Among the parameters affecting the total cost of distillation columns, the pressure is significantly important, as it affects components' activity, the reflux ratio, and the number of stages.

This work develops an efficient method for integrating the reaction and separation sections considering the auxiliary devices. The reactor model will be established based on the lumped model, and the column will be modeled with the combined shortcut and the rigorous model. A procedure based on the genetic algorithm will be proposed to solve the model efficiently. This manuscript is organized as follows: Section 2 will analyze the interaction between the reaction and distillation sections of the MTO process; in Section 3, the building of the optimization model is described, considering the optimization of the catalyst's coke content, reaction temperature, each column's operating pressure, and the allocation of utilities, etc. In Section 4, a case is studied to illustrate the application of the proposed method. The proposed method is summarized in the Conclusions section.

## 2. Interaction between the Reaction and Distillation Sections
MTO Process

The general MTO process with a front-end dethanizer is shown in Figure 1. In this process, the fluidized bed reactor (R1101) is the core of the entire process. The methanol, preheated to 300 °C, reacts quickly in the reactor, generating a significant amount of heat. Some coke will form and deposit on the catalysts' surface and cause the catalyst's deactivation. The deactivated catalyst is regenerated in regenerator R1102 to remove the coke. After preheating the methanol, the reactor effluent is sent to a quench column (T1101) and scrubber (T1102) to decrease its temperature and remove the water and catalyst. The high-temperature gas countercurrent makes contact with the water in column T1101. The gas product exiting the scrubber (T1102) mainly consists of low-carbon olefins (C_1–C_5).

The gas is compressed by compressors (C1101, C1102) in the separation section and then fed to the alkali column (T1103) to remove the oxides and acids. Then, it passes through the compressor (C1103), dryer (D1101), and inlets into the distillation sequence with five columns. The dethanizer (T1201) performs the split between C_2 and C_3. Its top product is separated in the demethanizer (T1202) and ethylene column (T1203) to remove C_1 and ethane, respectively, and pure ethylene is obtained at the top of T1203. The bottom product of T1201 is fed to the depropanizer (T1204) to separate C_3 from the top, which is further separated by the propylene column (T1205) to obtain pure propylene. The bottom product of T1204 consists of C_4 and C_5, and is sent out of the separating section.

In this process, the reactor effluent is separated in the separation section. The reactor parameters, such as feed composition, temperature, catalyst, etc., affect the product,

operation, and energy consumption of distillation columns. Optimizing the reaction and separation sections together is necessary to reduce energy consumption.
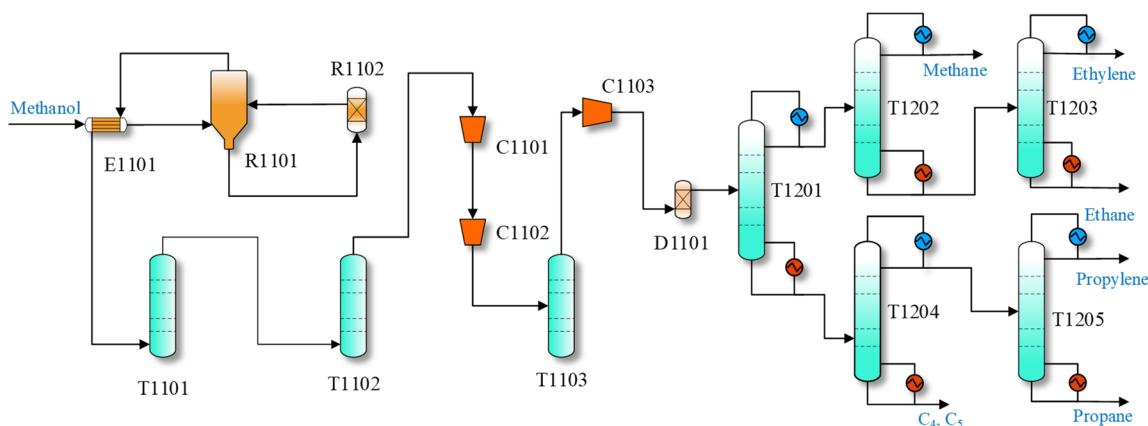
Figure 1. MTO process with front-end dethanizer.

In the reactor, methanol conversion and the selectivity to olefin are expected to be as high as possible. However, different parameters might have different influences on them. For example, the reaction rates and conversion increase along with the reactor's temperature. The selectivity to olefin depends on each reaction rate and their ratios, and its variation might be different. Furthermore, coke is formed at high temperatures, attaches to the catalyst's surface, and affects the catalyst's activity as well as the selectivity of desired products. Therefore, the reactor temperature (T) and coke content of the catalyst (C_C) are the key parameters influencing the products' flowrates and compositions. In the separation section, parameters such as the operating pressure, reflux ratio, and number of stages affect the total cost. The utilities selected for condensers and reboilers directly affect the heat exchange area and energy costs. For units arranged between two adjacent columns, such as heat exchangers, pumps, and valves, their expenses are related to the neighboring columns. These columns and auxiliary devices are affected by the feed of the separation section and, thus, the reactor parameters.

In this work, an efficient method is developed to integrate the reaction and separation sections. The reactor temperature (T) and the coke content of the catalyst (C_C) will be optimized together with the parameters of all distillation columns, considering the auxiliary devices arranged between two adjacent columns, such as heat exchangers, pumps, and valves. Both the energy cost and capital cost will be considered in the optimization. An MTO process is optimized based on the proposed method.

3. Optimization Model

3.1. Model of Physical Properties

Most of the components involved in the MTO process, such as methanol, ethylene, and propylene, have low polarity. The SRK equations can be used to estimate their P-V-T relations, and are shown in Equations (1)–(4). For mixtures, a_m and b_m, estimated based on the mixing rules shown in Equations (5) and (6), should be used in these equations instead of the a and b of pure components.

$$p = \frac{RT}{V-b} - \frac{a}{V(V+b)} \tag{1}$$

$$a = \frac{0.42748R^2T_c^2}{p_c}\left[1 + f_\omega\left(1 - \sqrt{T_r}\right)\right]^2 \tag{2}$$

$$f_\omega = 0.48 + 1.574\omega - 0.176\omega^2 \tag{3}$$

$$b = \frac{0.08664RT_c}{p_c} \tag{4}$$

$$a_m = \sum_i \sum_j x_i x_j \sqrt{a_i a_j}\left(1 - k_{i,j}\right) \tag{5}$$

$$b_m = \sum_i x_i b_i \tag{6}$$

where p_C is the critical pressure, T_C is the critical temperature, ω is the acentric factor, a and b are the relevant parameters, and $k_{i,j}$ is the binary interaction parameter.

The SRK equations can be solved efficiently with the compressibility factor (Z) introduced. Z equals $\frac{pV}{RT}$, and can be identified by solving the unitary cubic equation shown in Equation (7). One or two real solutions exist, and correspond to a single-phase or two-phase fluid, respectively.

$$f(Z) = Z^3 - Z^2 + \left(A - B - B^2\right)Z - AB = 0 \tag{7}$$

where $A = \frac{ap}{R^2T^2}$, $B = \frac{bp}{RT}$.

The vapor–liquid equilibrium (VLE) is the basis for the analysis and optimization of distillation. The fugacity of vapor and liquid can be calculated according to Equations (8)–(10).

$$f_i^V = f_i^L \tag{8}$$

$$f_i^V = p y_i \varphi_i^V \tag{9}$$

$$f_i^L = p x_i \varphi_i^L \tag{10}$$

where φ is the fugacity coefficient; p represents the system's pressure; and y_i and x_i are the mole fractions of component i in gas and liquid, respectively.

The fugacity coefficient can be obtained according to Equations (11)–(13). The gas–liquid equilibrium constant (K) and relative volatilities (α) are calculated by Equations (14) and (15), respectively.

$$\ln \varphi_i = \frac{b_i}{b_m}(Z - 1) - \ln(Z - B) + \frac{A}{B}\left(\frac{b_i}{b_m} - \delta_i\right)\ln\left(\frac{Z + B}{Z}\right) \tag{11}$$

$$\frac{b_i}{b_m} = \frac{T_i^c / p_i^c}{\sum_j x_j T_j^c / p_j^c} \tag{12}$$

$$\delta_i = \frac{2\sqrt{a_i}}{a_m}\sum_j x_j \sqrt{a_i}\left(1 - k_{i,j}\right) \tag{13}$$

$$K_i = \frac{y_i}{x_i} = \frac{\varphi_i^L}{\varphi_i^V} \tag{14}$$

$$\alpha_{i,j} = \frac{K_i}{K_j} = \frac{\varphi_i^L}{\varphi_i^V} \cdot \frac{\varphi_j^V}{\varphi_j^L} \tag{15}$$

Loads of condensers, reboilers, and heat exchangers are calculated according to the enthalpy difference of the involved stream. The enthalpy change at the real condition (ΔH) is the sum of that at the ideal value (ΔH^{id}) and deviation value (H^{R}). For each component, ΔH^{id} could be calculated based on Equation (16) [36], and H^{R} could be calculated by Equations (17) and (18).

$$\Delta H_i^{\mathrm{id}} = \left(a_i + b_i T + c_i T^2 + d_i T^3 + e_i T^4\right) R \cdot \Delta T \tag{16}$$

$$H^{\mathrm{R}} = \left(a_m - T\frac{\partial a_m}{\partial T}\right)\frac{1}{b_m}\ln\left(\frac{Z}{Z + B}\right) + RT(Z - 1) \tag{17}$$

$$\frac{\partial a_m}{\partial T} = -\frac{R}{2}\sqrt{\frac{0.42748}{T}}\sum_i\sum_j x_i x_j\left(1 - k_{i,j}\right)\left(f_{\omega,j}\sqrt{\frac{a_i T_j^c}{p_j^c}} + f_{\omega,i}\sqrt{\frac{a_j T_i^c}{p_j^c}}\right) \tag{18}$$

where a, b, c, d, and e are constants related to component i.

3.2. Model of Distillation

For a distillation column separating the mixture with m components, the material balance is shown by Equations (19) and (20). The minimum number of theoretical stages ($N_{\min}$) can be calculated according to the Fenske equation shown in Equation (21). The composition of products can be estimated based on Equation (22). The minimum reflux ratio can be calculated by the Underwood equation, which is shown in Equations (23) and (24) [37].

$$F = B + D \tag{19}$$

$$Fz_{i,F} = B_i x_{i,B} + D_i x_{i,D} \tag{20}$$

$$N_{\min} = \frac{\log\left(\frac{r_{l,D}}{1 - r_{l,D}} \cdot \frac{r_{h,B}}{1 - r_{h,B}}\right)}{\log(\alpha_{l,h})} \tag{21}$$

$$\frac{x_{i,D}}{x_{j,D}} = \alpha_{i,j}^{N_{\min}}\frac{x_{i,B}}{x_{j,B}} \tag{22}$$

$$\sum_{i=1}^{m}\frac{\alpha_{i,j}x_{i,F}}{\alpha_{i,j} - \theta} = 1 - q \tag{23}$$

$$R_{\min} + 1 = \sum_{i=1}^{m}\frac{\alpha_{i,j}x_{i,D}}{\alpha_{i,j} - \theta} \tag{24}$$

where q represents the feed condition, θ is the root of the Underwood equation, and its value lies between the relative volatilities of light and heavy key components.

The actual reflux ratio (R) and the number of theoretical stages (N) can be estimated according to the empirical formulas shown in Equations (25)–(29) [37].

$$R = R_F R_{\min} \tag{25}$$

$$Y = \frac{N - N_{\min}}{N + 1}, \quad X = \frac{R - R_{\min}}{R + 1} \tag{26}$$

$$Y = 0.2788 - 1.3154X + 0.4114X^{0.291} + 0.8268\ln X + 0.902\ln\left(X + \frac{1}{X}\right) \tag{27}$$

$$\frac{N_{rec}}{N_{stri}} = \left(\frac{B}{D}\frac{x_{h,F}}{x_{l,F}}\frac{x_{l,B}}{x_{h,D}}\right)^{0.206} \tag{28}$$

$$N = N_{rec} + N_{stri} + 1 \tag{29}$$

where R_F is the ratio of R to $R_{\min}$, and N_{rec} and N_{stri} are the numbers of theoretical stages in rectifying and stripping sections.

For each theoretical stage shown in Figure 2, the MESH equations shown by Equations (30)–(33) can be used to describe its material balances, equilibrium relationships, summation of compositions, and enthalpy balances [37].

$$0 = V_{j+1}y_{i,j+1} + L_{j-1}x_{i,j-1} + F_j z_{i,j} - \left(V_j + V_j'\right)_{i,j} - \left(L_j + L_j'\right)x_{i,j} \tag{30}$$

$$0 = y_{i,j} - K_{i,j}x_{i,j} \tag{31}$$

$$0 = \sum_{i=1}^{m}y_{i,j} - 1, \quad 0 = \sum_{i=1}^{m}x_{i,j} - 1 \tag{32}$$

$$0 = V_{j+1}H_{j+1}^{V} + L_{j-1}H_{j-1}^{L} + F_{j}H_{j}^{F} - \left(V_{j} + V_{j}'\right)H_{j}^{V} - \left(L_{j} + L_{j}'\right)H_{j}^{V} - Q_{j} \tag{33}$$

where V and L are the flowrates (kmol·h^{-1}) of vapor and liquid through the plates; V' and L' are the flowrates (kmol·h^{-1}) of vapor and liquid leaving the column; subscript i and j are component and theoretical stage, respectively; the first stage is the condenser; and the last stage is the reboiler. H and Q are enthalpy (kW) and heat load (kW), respectively.
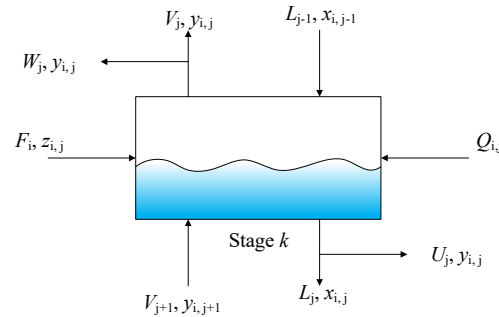
Figure 2. Schematic diagram of the theoretical stage.

3.3. Models of Optimization

3.3.1. Evaluation of Distillation Columns

In this work, the total annual cost (*TAC*), which includes the operating cost (C_{ope}) and the capital cost (C_{cap}), is used to evaluate the columns. The operating cost consists of steam, cooling water, electricity, etc. The capital cost mainly includes that of the columns and heat exchangers, while the costs of the other units are much lower and only change slightly during the optimization; hence, they are neglected. The TAC is calculated by Equation (34).

$$TAC = C_{ope} + \frac{C_{cap}}{PBP} \tag{34}$$

where *PBP* is the payback period, and the operating cost is determined by the total energy consumption (C_i) and the utility price (Q_i). C_{ope} is calculated by Equation (35).

$$C_{ope} = AOT \cdot \sum C_i Q_i \tag{35}$$

C_{cap} includes the expenses of shells (C_{shell}) and plates (C_{plate}), and can be estimated by Equations (36)–(40) [38].

$$C_{shell} = 17640 \cdot D_c^{1.066} \cdot H_c^{0.802} \tag{36}$$

$$C_{plate} = 229 \cdot D_c^{1.55} \cdot \frac{N}{\eta} \tag{37}$$

$$D_c = \left[\frac{4}{\pi v} \cdot D \cdot (R+1) \cdot 22.4 \cdot \frac{T_D}{273} \cdot \frac{1}{P} \cdot \frac{1}{3600} \right]^{0.5} \tag{38}$$

$$v = 0.761 \cdot \left(\frac{1}{P} \right)^{0.5} \tag{39}$$

$$H_c = 0.61 \cdot \frac{N}{\eta} + 4.27 \tag{40}$$

where D_c is the diameter of column (m); H_c is the height of column (m); v is the vapor velocity (m·s^{-1}); T_D is the top temperature (K); P is the operating pressure (atm); N is the number of theoretical stages; and η is the Murphree's plate efficiency.

The capital costs of heat exchangers (C_{hex}), including condensers and reboilers, are estimated based on the heat exchange area, as shown in Equations (41) and (42).

$$C_{\text{hex}} = 7269 \cdot A^{0.65} \tag{41}$$

$$Area = \frac{Q}{U \cdot LMTD} \tag{42}$$

where *Area* represents the heat exchange area (m^2), and *LMTD* is the logarithmic mean temperature difference, which can be calculated by Equations (43)–(45). *U* is the overall coefficient of heat transfer (kW·°C^{-1}·m^{-2}), and its value depends on the properties of both hot and cold streams. The heat transfer coefficients for different media are shown in Table 1.

$$LMTD = [(\Delta T_1 \cdot \Delta T_2) \cdot (\Delta T_1 + \Delta T_2)/2]^{\frac{1}{3}} \tag{43}$$

$$\Delta T_1 = T_{\text{H,out}} - T_{\text{C,in}} \tag{44}$$

$$\Delta T_2 = T_{\text{H,in}} - T_{\text{C,out}} \tag{45}$$

where ΔT_1 and ΔT_2 are the temperature differences at the cold and hot ends; $T_{\text{H,in}}$ and $T_{\text{H,out}}$ are the inlet and outlet temperatures of the hot stream; and $T_{\text{C,in}}$ and $T_{\text{C,out}}$ are the inlet and outlet temperatures of the cold stream.

Table 1. Heat transfer coefficients for different mediums.

Types of Fluid	U (kW·°C^{-1}·m^{-2})
Gas—Gas	0.17
Gas—Condensing gas	0.28
Gas—Evaporating liquid	0.28
Liquid—Liquid	0.57
Liquid—Condensing gas	0.85
Liquid—Evaporating liquid	0.85

3.3.2. Optimization of Distillation Columns

For distillation columns, their performance and energy consumption are affected by the number of stages (*N*), reflux ratio (*R*), pressure (*p*), feed location (N_f), etc. These parameters can be optimized simultaneously based on a rigorous model. However, the optimization is a complex MINLP problem; its solving is difficult and time-consuming. Sometimes, infeasible solutions might be obtained, especially for the simultaneous optimizations of multiple columns. Both shortcut and rigorous models are applied in this work to increase the efficiency and accuracy of the optimization. The operating pressure of each column is optimized, and the detailed optimization steps are shown in Figure 3.

In this procedure, the relative volatilities are calculated by SRK equations, and the shortcut model is applied to estimate *N*, *R*, and N_f. The rigorous model is used to obtain the detailed parameters of the column. The combination of shortcut and rigorous models is an integrated consideration of the calculation speed and accuracy, and it has advantages over using either method alone. The TAC of the column is estimated based on the equations introduced in Section 3.3.1. In the procedure, the appropriate heating and cooling utilities are selected automatically based on the limitation of the minimum temperature difference between the cold and hot streams. The utilities are divided into different grades according to their prices. For streams that need to be cooled or heated, inexpensive utilities are preferred. They are selected according to the temperatures of the streams as well as the temperature differences between the streams and utilities. When the operating pressure of each column is set, the TAC of the entire separation section can be calculated, and the optimal operating pressures corresponding to the minimum TAC can be targeted based on the genetic algorithm.
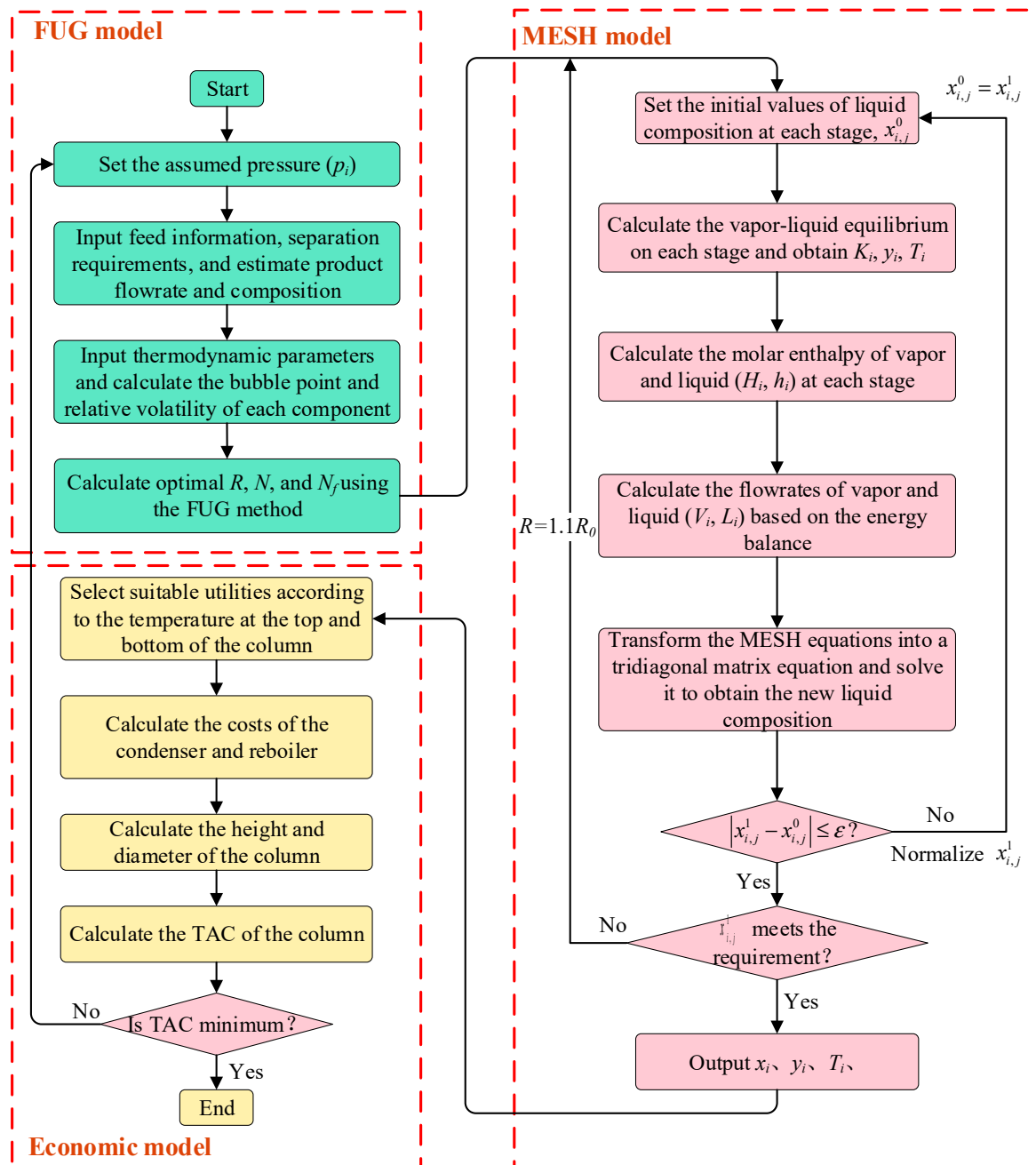
Figure 3. Optimization steps of a column.

3.3.3. Optimization of Reaction—Distillation System

In the optimization of the reaction–distillation system, the influences of reactor and distillation parameters on the flowrates and compositions of products are considered, as well as the TAC of the columns and other devices. The seven-lumped kinetic model proposed by Ying [11] is used to predict the reactor performance and the influence of reactor parameters. The lumped components are CH_4, C_2H_4, C_3H_6, C_3H_8, C_4, C_5, and coke. The lumped component CH_4 contains a small amount of H_2, CO, and CO_2; the lumped component C_5 contains some ethane. The formation rate of seven lumped components is shown in Equation (46) [11]. Water is generated simultaneously, and its formation rate is shown in Equation (47).

$$r_i = \nu_i k_i \theta_W \phi_i C_{\text{MeOH}} M_i \tag{46}$$

$$r_{\text{H}_2\text{O}} = \sum_{i=1}^{7} k_i \theta_W C_{\text{MeOH}} M_{\text{H}_2\text{O}} \tag{47}$$

where i (i = 1, 2, ... , 7) refers to the lumped components, which are CH_4, C_2H_4, C_3H_6, C_3H_8, C_4, C_5, and coke, respectively. r_i ($g \cdot g_{\text{cat}}^{-1} \cdot \min^{-1}$) represents the formation rate of component i. ν_i is the stoichiometric number, and their values are 1, 1/2, 1/3, 1/3, 1/4, 1/5, and 1, respectively. k_i is the kinetic constant of component i, as shown in Equation (48). θ_W is the parameter describing the influence of water. ϕ_i is a parameter reflecting the catalyst deactivation, as shown in Equation (52). C_{MeOH} is the concentration of methanol ($\text{mol} \cdot \text{L}^{-1}$), and M_i is the molecular weight of component i.

$$k_i = k_{i0} \exp\left[-\frac{E_{a,i}}{R}\left(\frac{1}{T} - \frac{1}{723.5}\right)\right] \tag{48}$$

$$\phi_i = \frac{1}{1 + A \exp(B(100C_C - D))} \exp(-100\beta_i C_C) \tag{49}$$

where k_{i0} is the kinetic constant in the reference state; $E_{a,i}$ is the activation energy. A, B, D, and β_i are empirical values and can be found in Ying's work [11]. C_C is the coke content of the catalyst.

In the actual MTO processes developed by DICP, the conversion of methanol is greater than 99% [5], and is taken as 1 in this study to simplify the optimization. The reaction products consist of hydrocarbons, coke, and water. According to the reaction rate of methanol, the mole fractions ($z_{mole,i}$) of the lumped components are shown in Equation (50). The total flowrate of the seven lumped components (F_r, $\text{kmol} \cdot \text{h}^{-1}$) can be identified based on Equation (51). The coke is removed after leaving the reactor; the mole fraction (z_i) and flowrate (F, $\text{kmol} \cdot \text{h}^{-1}$) of the stream inlet into the separation section are calculated by Equations (52) and (53).

$$z_{mole,i} = \frac{r_i / M_i}{\sum\limits_{i=1}^{7} r_i / M_i} = \frac{\nu_i k_i \phi_i}{\sum\limits_{i=1}^{7} \nu_i k_i \phi_i} \tag{50}$$

$$F_r = \frac{F_0}{\sum\limits_{i=1}^{7} \frac{z_{mole,i}}{\nu_i}} \tag{51}$$

$$z_i = \frac{r_i / M_i}{\sum\limits_{i=1}^{6} r_i / M_i} = \frac{\nu_i k_i \phi_i}{\sum\limits_{i=1}^{6} \nu_i k_i \phi_i} \tag{52}$$

$$F = F_r \cdot \sum_{i=1}^{6} z_{mole,i} \tag{53}$$

The yield of component i (Y_i) equals the flowrate of i ($\text{g} \cdot \text{s}^{-1}$) in the products when unit methanol (1 $\text{g} \cdot \text{s}^{-1}$) is consumed. As methanol converts at a rate of nearly 100%, the consumption rate of methanol equals the sum of the lumped components and water. Y_i is calculated by Equation (54).

$$Y_i = \frac{r_i}{\sum\limits_{i=1}^{7} r_i + r_{\text{H}_2\text{O}}} = \frac{\nu_i k_i \phi_i M_i}{\sum\limits_{i=1}^{7} k_i \phi_i (\nu_i M_i + M_{\text{H}_2\text{O}})} \tag{54}$$

The reaction temperature (T) and coke content of the catalyst (C_C) influence the distillation system. T can be controlled by adjusting the flowrates of utilities. C_C can be controlled by adjusting the temperature or flowrate of the gas inlet into the regenerator.

In the separation section, multiple distillation columns interact with each other. Some auxiliary devices, such as heat exchangers, pumps, and valves, are used to guarantee the

feed conditions in order to satisfy the requirement. These units are related to two adjacent columns, and will be selected automatically in the optimization. For example, when both the pressure and temperature of the downstream column are higher than those of the upstream one, a pump and heater should be used to pressurize and preheat the stream connecting these two columns. On the contrary, the valve and cooler should also be placed.

The TAC of these auxiliary devices is calculated based on the following simplifications: (1) the feed of each column is saturated liquid; (2) the temperature of the stream is unchanged when passing through pumps or valves; (3) the heat load of these units equals the enthalpy changes of the related streams. The electricity consumed by the pump is calculated by Equation (55).

$$W_{\mathrm{e}} = \frac{F_{\mathrm{feed}} \cdot AOT \cdot (H_{\mathrm{feed},2} - H_{\mathrm{feed},1})}{3600 \cdot \eta_{\mathrm{pump}}} \tag{55}$$

where W_{e} is the annual electricity consumption (kWh); F_{feed} is the feed flowrate (kmol·h^{-1}); AOT is the annual operating time (h); H_{feed} is the enthalpy of feed; subscripts 1 and 2 are the inlet and outlet streams, respectively; and η_{pump} is the efficiency of the pump.

In the MTO process, the expected products are ethylene and propylene, and the byproducts are other hydrocarbons and coke. The total yield of ethylene and propylene is usually maximized in the practical plant. However, different processes might have different ethylene-to-propylene ratios and energy consumption. Maximizing the total yield of ethylene and propylene cannot guarantee that the minimum TAC will be achieved. The total yield of the target products and the TAC should be considered simultaneously in order to optimize the MTO processes. In this work, the models of reaction and distillation sections are integrated to optimize the reaction and distillation sections. The object is to maximize the profit calculated by Equation (56). In this equation, the capital and energy costs of the reaction section are not considered, as they change slightly according to the coke content and are not affected by the pressure of distillation columns.

$$P = P_{\mathrm{sale}} - TAC - P_{\mathrm{material}} - P_{\mathrm{other}} \tag{56}$$

where P represents the annual profit (USD/year); P_{sale} is the revenue of target products (USD/year); TAC is the total annual cost of the distillation section; P_{material} is the cost of methanol (USD/year); and P_{other} is the total cost of others, which has little influence on the system and is taken unchanged.

The primary optimization steps are listed below:

(1)   Calculate the flowrate and composition of the products.
(2)   Estimate the flowrates and compositions of the feed and product according to the separation requirements and mass conservation.
(3)   Optimize columns according to the steps mentioned in Section 3.3.2, and target optimal parameters and utilities.
(4)   Select the units between adjacent columns and calculate their TACs.
(5)   Calculate the profit of the MTO process.

The genetic algorithm can optimize the operating pressures and reaction parameters until the profit is at its maximum.

Based on this procedure, the reaction and separation sections can be integrated, considering the market prices of products, the allocation of utilities, the total cost of the distillation system, and auxiliary devices together, and the profit can be maximized.

4. Case Study

4.1. Optimization of Distillation Columns

In this section, the distillation columns shown in Figure 1 are optimized based on the shortcut and rigorous models in terms of minimizing the TAC. In the reactor model, T and C_{C} were taken as 490 °C and 7.0%, respectively. The lumped component C_5 consisted of

equimolar n-butene and ethane; the lumped component C_4 was taken as i-butylene. The reactor effluent was sent to the distillation system after the coke and water were removed; its flowrate was 2456.1 kmol·h^{-1}, and the composition is shown in Table 2. The parameters of each lumped component are listed in Appendix A, including binary interaction parameters, critical temperature, critical pressure, Pitzer eccentricity factor, Antoine constants, and correlation parameters of enthalpy.

Table 2. Feed composition of the separation section.

Components	CH_4	C_2H_4	C_2H_6	C_3H_6	C_3H_8	$i\text{-}C_4H_8$	$n\text{-}C_5H_{10}$
Molar fraction	0.0685	0.5460	0.0080	0.2943	0.0170	0.0583	0.0080

In the optimization, the payback period (*PBP*) was set as three years, the total production time (*AOT*) was 8000 h per year, and the prices of utilities are listed in Table 3. When selecting the utilities, the minimum temperature difference between the cold and hot streams was set as 5 °C.

$$C_{\text{ope}} = AOT \cdot \sum C_i Q_i \tag{57}$$

Table 3. Prices of different utilities.

| Utility	Inlet Temperature (°C)	Outlet Temperature (°C)	Abbreviation	Price ($·GJ^{-1})
Refrigerant (Ethylene)	−101 (l)	−101 (g)	RE	21
Refrigerant (Propylene)	−50 (l)	−50 (g)	−50 RP	13.11
Refrigerant (Propylene)	−35 (l)	−35 (g)	−35 RP	10.6
Refrigerant (Propylene)	−20 (l)	−20 (g)	−20 RP	8.2
Chilled water	5	15	CHW	4.43
Cooling water	25	35	CW	0.354
Quench water	120	90	QW	0.445
LP-steam	160 (g)	160 (l)	LP	7.78
Electricity	-	-	EL	16.8

The dethanizer (T1201) was selected to verify the accuracy of the distillation model mentioned in Section 3. The operating pressure was initially set as 2800 kPa. The calculation began with the shortcut model shown by Equations (19)–(24), and the minimum reflux ratio and the number of theoretical stages were identified to be 0.48 and 22.8, respectively. Based on Equations (25)–(29), the operational reflux ratio (*R*), the number of theoretical stages (*N*), and the feed stage were identified to be 0.57, 60, and 22, respectively. With these parameters taken as the initial values, each stage's liquid composition ($x_{i,j}$) was identified according to the steps listed in Figure 3. The *R*, *N*, and feed stages of T1201 were determined to be 0.74, 60, and 22, and other detailed parameters were obtained. The selected heating and cooling utilities were quench water and propylene refrigerant (−50 °C), respectively. The TAC was USD 2.797 × 10^6, and the total capital and annual operating costs were USD 1.135 × 10^6 and USD 2.418 × 10^6, respectively.

Matlab 2020b software was used to perform the calculation, and the results were obtained in 4 s (Computer configuration: Windows 10 64-bit operating system; Intel(R) Core (TM) I5-7500 CPU @ 3.40GHz). The obtained distillation parameters were input into Aspen Plus software and simulated based on the Radfrac module. The errors between the simulation results and those obtained by the proposed method were less than 6%, as shown in Table 4. Thus, the results identified by the proposed method are accurate.

The detailed parameters and cost changed along with the operating pressure. The parameters and costs of the separation section were optimized at different pressures, and the dethanizer's minimum cost is shown in Figure 4.

Table 4. Comparison of results obtained by the proposed methods and rigorous simulation.

|	Proposed Method	Aspen Plus	Error
Recovery of ethane	0.99	0.9512	4.1%
Recovery of ethylene	0.9999	0.9999	0
Recovery of propylene	0.999	0.9956	0.3%
Top temperature/°C	−31.8	−31.3	−1.6%
Bottom temperature/°C	74.7	74.9	−0.3%
Duty of condenser/kW	6129	6491	−5.6%
Duty of reboiler/kW	8117	8621	−5.8%
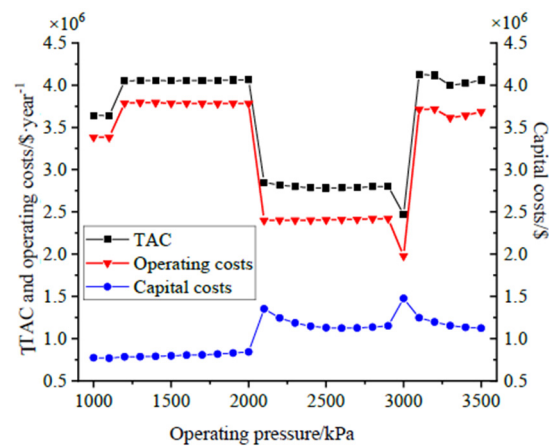
Figure 4. The costs of the dethanizer at different pressures.

Due to the changes of utilities according to the operating pressure of columns, there were sharp changes in the curves corresponding to TAC, operating cost, and capital cost. In Figure 4, there are two sharp changes with a large margin. One lies in the pressure interval of 2000 kPa~2100 kPa, and the other corresponds to the pressure of 3000 kPa. When the pressure was lower than 2000 kPa, the top temperature of the dethanizer was lower than −46.4 °C, and in this case, the cooling utility of the condenser should be ethylene (liquid, −101 °C). Otherwise, the heat transfer temperature difference was lower than the minimum value (5 °C). When the pressure was increased to 2100 kPa, the top temperature rose to −44.4 °C, and in this scenario, the cooling utility can be replaced by propylene (liquid, −50 °C), which is cheaper and leads to lower energy costs. At the same time, the heat transfer area increases, leading to higher capital costs. When the pressure was 2900 kPa, the top and bottom temperatures were −30.2 °C and 76.6 °C, and the cooling and heating utilities in this case should be propylene (−50 °C) and quench water, respectively. When the pressure rose to 3000 kPa, the top temperature reaches −28.6 °C, and the cheaper propylene refrigerant (−35 °C) can be selected in this case. Correspondingly, the annual operating cost was reduced, and the capital cost was increased. When the pressure rose to 3100 kPa, the bottom temperature rose to 80.4 °C, and since quenched water cannot be used as a heating utility, the more expensive LP-steam should be used here. Hence, the annual operating cost increased, and the capital cost decreased. The changes in the heating and cooling utilities in different pressure ranges are shown in Table 5.

Table 5. The heating and cooling utilities in different pressure ranges.

Pressure/kPa	1000~2000	2100~2900	3000	3100~3500
Cooling utility	RE	−50 RP	−35 RP	−35 RP
Heating utility	QW	QW	QW	LP

For other columns of the distillation section, the changes in the costs along with the operating pressures are shown in Figure 5.
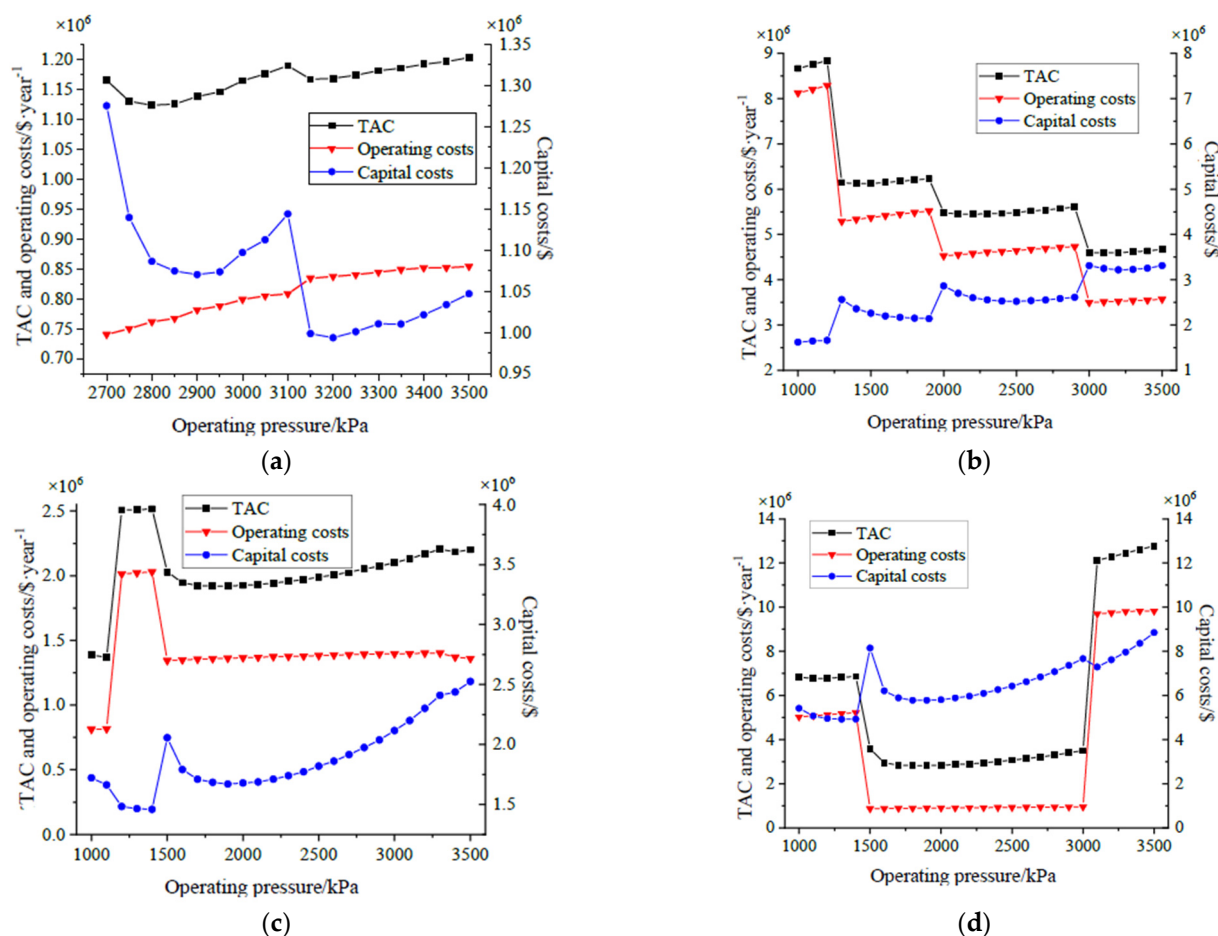
Figure 5. Changes of costs according to the operating pressure: (**a**) demethanizer; (**b**) ethylene column; (**c**) depropanizer; (**d**) propylene column.

According to Figures 4 and 5, the optimal operating pressures of the five columns could be identified based on the models introduced in Section 3. In the optimization, not only the column parameters (such as operating pressures, reflux ratio, the number of stages) were considered, but also the selection of utilities for the condensers and reboilers. The optimal results are listed in Table 6. With these columns optimized, the TAC of the separation section (including the units between the columns) was 1.27×10^7 USD/year, and the profit of the process was 5.47×10^7 USD/year.

4.2. Optimization for Reaction–Distillation System

The reaction and separation systems are optimized simultaneously to maximize the profit and target the corresponding parameters. The decision variables are reaction temperature (T), coke content of catalyst (C_C), and the operating pressures of the dethanizer (p_1), demethanizer (p_2), ethylene column (p_3), depropanizer (p_4), and propylene column (p_5). The reactor temperature and coke content should satisfy $450\,°C \le T \le 550\,°C$, $3\% \le C_C \le 7.8\%$. Otherwise, the formation rates of main products will decrease. The operating pressure constraints are selected according to the actual MTO process: $800\,kPa \le p_1 \le 3500\,kPa$, $2700\,kPa \le p_2 \le 3500\,kPa$, $800\,kPa \le p_3 \le 3500\,kPa$, $800\,kPa \le p_4 \le 2500\,kPa$, and $800\,kPa \le p_5 \le 2500\,kPa$. The prices of the products are taken as the average values in the past year in China, which are 1227 USD/t for ethylene and 1242 USD/t for propylene, respectively. The price of methanol is the production cost from coal to methanol, 343 USD/t.

Table 6. Optimal parameters of columns.

Parameters	T1201	T1202	T1203	T1204	T1205
Operating pressure/kPa	3000	2800	3100	1100	1800
Top temperature/°C	−28.6	−98.3	−12.4	23.3	43.3
Bottom temperature/°C	78.5	−15.6	10.7	78.6	53.9
Reflux ratio	0.82	4.91	4.86	0.95	14.77
Number of stages	62	46	146	83	121
Feed stage	23	2	124	44	52
Duty of condenser/kW	6137	1206	14,988	5872	38,533
Duty of reboiler/kW	8152	1579	14,975	5624	38,616
Cooling utilities	−35 RP	RE	−20 RP	CHW	CW
Heating utilities	QW	QW	QW	QW	QW
Capital cost/USD 10^6	1.4739	1.1395	3.2479	1.6632	5.7811
Operating cost/10^6 USD/year	1.9780	0.7499	3.5112	0.8162	0.8878
TAC/10^6 USD/year	2.4693	1.1297	4.5939	1.3706	2.8148

The influences of the two reaction parameters on the reaction–separation system were studied. With the reactor temperature taken as 450 °C, 470 °C, 490 °C, 510 °C, 530 °C, and 550 °C, and with C_C taken as 0.03, 0.04, 0.05, 0.07, and 0.078, respectively, the reaction–separation system's profit and the minimum TACs of separation section were obtained, and are shown in Figure 6.
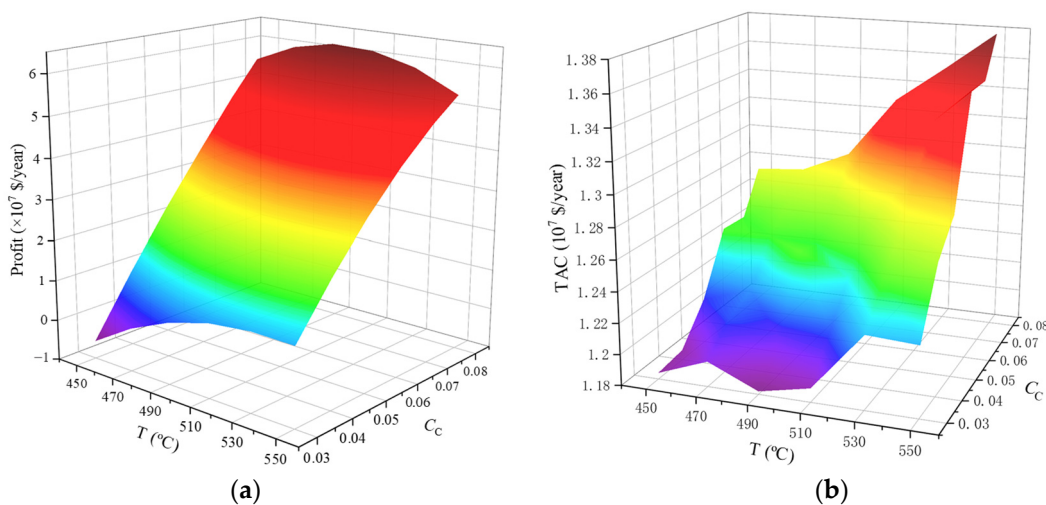
Figure 6. The maximum profit and the minimum TAC at different reaction parameters. (**a**) Maximum profit of the reaction–separation system (**b**) Minimum TAC of separation section.

Figure 6 shows that the profit is negative when T is lower than 450 °C, and C_C is less than 3%. With the increment of T, the profit of the MTO process increases at first and then decreases. The maximum profit is achieved when T lies between 490 °C and 510 °C. In addition, with the increment of T and C_C, the minimum TAC of the separation section has an increasing trend overall, although it may fluctuate locally. This is because the minimum TAC of the separation section is significantly affected by the distillation parameters, some of which are discontinuous variables, such as the number of stages, feed position, and utilities.

At different reaction conditions (T and C_C), the optimal operating pressures are different, and these are listed in Appendix B. These data show that the optimal pressures change slightly and remain within a certain range at different reaction conditions: 2540 kPa $\leq p_1 \leq$ 3127 kPa, 2759 kPa $\leq p_2 \leq$ 3303 kPa, 2972 kPa $\leq p_3 \leq$ 3345 kPa, 893 kPa $\leq p_4 \leq$ 1146 kPa, and 1763 kPa $\leq p_5 \leq$ 2113 kPa.

In order to obtain the optimum reaction and distillation parameters more accurately, a genetic algorithm was used to optimize the reaction–distillation system. The genetic algorithm was configured as follows: fitness function—Equation (54); max iterations—40; mutation—0.2; crossover fraction—0.8. Matlab® was used to solve the problem, and the total calculating time was 5 h. The optimal reaction temperature and catalyst's coke content were identified to be 496 °C and 7.8%, respectively. The maximum profit was 6.28×10^7 USD/year, 15.3% greater than that identified in Section 4.1; the minimum TAC of the separation section was 1.29×10^7 USD/year (including the costs of the units lying between the columns), 3.73% less than that identified in Section 4.1. Other optimal parameters are listed in Table 7.

Table 7. Distillation parameters corresponding to the maximum profit.

Parameters	Dethanizer	Demethanizer	Ethylene Column	Depropanizer	Propylene Column
Operating pressure/kPa	3051	3058	3167	1134	1934
Top temperature/°C	−29.9	−95.6	−11.5	24.5	46.6
Bottom temperature/°C	79.2	−12.0	11.7	79.9	57.2
Reflux ratio	0.76	4.80	4.98	0.96	15.4
Number of stages	62	49	149	84	126
Feed stage	23	2	128	44	54
Duty of condenser/kW	6342	1311	15,717	5678	37,669
Duty of reboiler/kW	8390	1750	15,694	5456	37,749
Cooling utilities	−35 RP	RE	−20 RP	CHW	CW
Heating utilities	QW	QW	QW	LP	QW
Capital cost/USD 10^6	1.5822	1.0198	3.2615	1.6485	5.7462
Operating cost/10^6 USD/year	2.0436	0.8154	3.6821	0.7895	0.8678
TAC/10^6 USD/year	2.5710	1.1554	4.7693	1.3390	2.7832

Comparing the optimization results of the reaction–distillation system with those obtained in Section 4.1, it is evident that simultaneous optimization of the reaction and separation sections can result in a better outcome.

5. Conclusions

For the reaction and separation sections of the MTO process, a framework was developed for the simultaneous design and optimization of the reaction and distillation sections. Multiple parameters were able to be optimized simultaneously to target the minimum TAC and maximum profit. With the shortcut and rigorous distillation models combined, the separation section could be analyzed and optimized efficiently, with detailed column parameters identified, utilities selected, and the TAC minimized. The integration of the reaction and separation sections could consider the reactor parameters, the market prices of products, and the total cost of the distillation system and auxiliary devices together, and thus maximize the profit. For the studied MTO process, the reactor temperature and catalyst's coke content were optimized, together with the column pressure and each column's utility, using a genetic algorithm. Their optimal values were 496 °C and 7.8%, respectively. The maximum profit was 6.24×10^7 USD/year, 15.3% greater than that identified with only the separation section optimized, and the minimum TAC of the separation section was 3.73% less.

Data Availability Statement: Not applicable.

Conflicts of Interest: The authors declare no conflict of interest.

Nomenclature

a, b	the relevant parameters of the component
a_m, b_m	the relevant parameters of the mixture
Area	the heat exchange area (m^2)
AOT	the annual operating time (h)
C_C	coke content of the catalyst
C_{cap}	capital cost (USD/year)
C_{hex}	capital costs of heat exchanger (USD/year)
C_i	total energy consumption (kW)
C_{MeOH}	the concentration of methanol ($mol \cdot L^{-1}$)
C_{ope}	operating cost (USD/year)
C_{plate}	the expenses of plates (USD/year)
C_{shell}	the expenses of shell (USD/year)
D_c	the diameter of column (m)
$E_{a,I}$	the activation energy ($J \cdot mol^{-1}$)
f^L	fugacity of liquid
f_i^V	fugacity of vapor
F	flowrate of the stream inlet into the separation section ($kmol \cdot h^{-1}$)
F_{feed}	the feed flowrate ($kmol \cdot h^{-1}$)
F_r	total flowrate of the seven lumped components ($kmol \cdot h^{-1}$)
H	enthalpy (kW)
H^R	deviation value of enthalpy (kW)
H_c	the height of column (m)
H_{feed}	the enthalpy of feed
k_i	the kinetic constant of component i
k_{i0}	kinetic constant at the reference state
$k_{i,j}$	binary interaction parameter
K	gas–liquid equilibrium constant
L	flowrate of liquid through the plate, $kmol \cdot h^{-1}$
L'	flowrate of liquid leaving the column, $kmol \cdot h^{-1}$
LMTD	the logarithmic mean temperature difference, K
M_i	the molar mass of component i
N	the number of theoretical stages
p	pressure (kPa)
P	represents the annual profit (USD/year)
$P_{material}$	the cost of methanol (USD/year)
P_{sale}	the revenue of target products (USD/year)
PBP	the payback period (year)
q	feed condition
Q	heat load (kW)
Q_i	the utility price ($USD \cdot GJ^{-1}$)
r_i	the formation rate of component I ($g \cdot g_{cat}^{-1} \cdot min^{-1}$)
R	reflux ratio
R_F	the ratio of R to R_{min}
T	temperature (K)
T_D	top temperature (K)
TAC	the total annual cost of the distillation section (USD/year)
U	the overall coefficient of heat transfer ($kW \cdot {}^{\circ}C^{-1} \cdot m^{-2}$),
v_I	the stoichiometric number
V	flowrate of vapor through the plate, $kmol \cdot h^{-1}$
V'	flowrate of vapor leaving the column, $kmol \cdot h^{-1}$
W_e	the annual electricity consumption (kWh)
y_i, x_i	the mole fractions of component i in gas and liquid, respectively.
Y_i	yield of component i

z_i	the mole fractions of the stream inlet into the separation section	
Z	compressibility factor	
α	relative volatility	
ΔH	enthalpy change (kW)	
ΔT_1	temperature difference at the hot end (K)	
ΔT_2	temperature difference at the cold end (K)	
η	Murphree plate efficiency	
η_{pump}	pump's efficiency	
θ	the root of the Underwood equation	
θ_{W}	parameter describing the influence of water content in the feed	
ν	the vapor velocity in the column (m·s^{-1})	
φ	the fugacity coefficient	
ϕ_i	parameter reflecting the catalyst deactivation	
ω	the acentric factor	

Subscripts

c	critical state
C	cold stream
H	hot stream
i	component
in	inlet stream
j	theoretical stage
out	outlet stream
rec	rectifying section
stri	stripping section

Superscript

id	ideal state

Appendix A

Table A1. Binary interaction parameters.

	CH$_4$	C$_2$H$_4$	C$_2$H$_6$	C$_3$H$_6$	C$_3$H$_8$	i-C$_4$H$_8$	n-C$_5$H$_{10}$
CH$_4$	0	0.01	0.01	0.021	0.023	0.0275	0.041
C$_2$H$_4$	0.01	0	0	0.003	0.0031	0.004	0.006
C$_2$H$_6$	0.01	0	0	0.003	0.0031	0.004	0.006
C$_3$H$_6$	0.021	0.003	0.003	0	0	0.003	0.0045
C$_3$H$_8$	0.023	0.0031	0.0031	0	0	0.003	0.0045
i-C$_4$H$_8$	0.0275	0.004	0.004	0.003	0.003	0	0.0008
n-C$_5$H$_{10}$	0.041	0.006	0.006	0.0045	0.0045	0.008	0

Table A2. Thermodynamic parameters of each component.

Parameters	CH$_4$	C$_2$H$_4$	C$_2$H$_6$	C$_3$H$_6$	C$_3$H$_8$	i-C$_4$H$_8$	n-C$_5$H$_{10}$
T_c/K	190.56	282.34	305.32	364.90	369.83	407.85	469.70
p_c/bar	45.99	50.41	48.72	46.00	42.48	36.40	33.70
ω	0.011	0.087	0.099	0.142	0.152	0.186	0.252
A	5.964	6.402	6.107	6.651	6.809	6.274	5.969
B	438.5	800.9	720.8	1186	1348	1095	1044
C	−0.9394	14.04	−8.924	32.00	53.76	−9.441	−39.70
H_0/kJ·kmol^{-1}	−75,402	51,461	−85,110	18,650	−106,481	−137,353	−149,685
a	4.568	4.221	4.178	3.834	3.847	3.351	7.554
$b \times 10^3$	−8.975	−8.782	−4.227	3.893	5.131	17.883	−0.368
$c \times 10^5$	3.631	5.795	5.660	4.688	6.011	5.477	11.85
$d \times 10^8$	−3.047	−6.729	−6.651	−6.013	−7.893	−8.009	−14.94
$e \times 10^{11}$	1.091	2.511	2.487	2.283	3.079	3.243	5.753

Appendix B

Table A3. Detailed results at different T and C_C values.

T	C_C	Profit (10^7 $/Year$)	Min TAC (10^7 $/Year$)	p_1 (kPa)	p_2 (kPa)	p_3 (kPa)	p_4 (kPa)	p_5 (kPa)
450	3.0%	−0.56	1.18	2540	2841	3345	916	1973
470	3.0%	0.07	1.20	2600	2896	3051	1120	1796
490	3.0%	0.52	1.18	2828	2890	3033	1109	1855
510	3.0%	0.82	1.19	2888	2879	3023	998	1763
530	3.0%	0.93	1.23	2832	3139	3090	981	1814
550	3.0%	0.92	1.23	2780	2840	3094	1036	1790
450	4.0%	0.88	1.19	2592	2768	3116	1056	1866
470	4.0%	1.47	1.21	2841	2835	3053	998	1856
490	4.0%	1.90	1.20	2866	2894	2972	1017	1827
510	4.0%	2.15	1.21	2984	3072	3191	1018	1839
530	4.0%	2.21	1.25	2967	3040	3201	1093	2013
550	4.0%	2.12	1.26	3069	3169	3214	993	1778
450	5.0%	2.22	1.21	2552	2941	3257	1129	1835
470	5.0%	2.79	1.22	2745	2998	3035	1015	2011
490	5.0%	3.16	1.25	2871	3021	2978	893	1879
510	5.0%	3.38	1.24	3007	3079	3131	1113	1788
530	5.0%	3.37	1.27	3056	3198	3246	1016	1918
550	5.0%	3.19	1.28	3061	3104	3117	1045	1853
450	6.0%	3.47	1.25	2642	2759	3238	901	1809
470	6.0%	4.02	1.25	2762	2947	3086	987	1903
490	6.0%	4.36	1.24	3013	3015	3159	1014	1808
510	6.0%	4.50	1.26	3061	2996	3145	1117	1787
530	6.0%	4.40	1.30	2966	3041	3036	1107	1769
550	6.0%	4.11	1.35	3082	3193	3186	1033	1844
450	7.0%	4.67	1.25	2670	2994	3049	1146	1886
470	7.0%	5.16	1.26	2892	2951	3174	1118	1814
490	7.0%	5.44	1.27	3007	2990	3076	1129	1793
510	7.0%	5.45	1.32	2823	2934	2975	1050	1865
530	7.0%	5.30	1.32	3060	3109	3146	1099	1831
550	7.0%	4.89	1.35	3077	3303	3341	1075	1924
450	7.8%	5.55	1.27	2827	2903	3127	945	1796
470	7.8%	6.00	1.28	2960	3104	3150	1000	1934
490	7.8%	6.22	1.29	2970	3223	3150	1100	1928
510	7.8%	6.17	1.33	2939	2927	3075	1050	1867
530	7.8%	5.95	1.35	2987	2927	3074	1049	1867
550	7.8%	5.41	1.38	3127	3280	3200	1106	2113

References

1. Gogate, M.R. Methanol-to-olefins process technology: Current status and future prospects. *Pet. Sci. Technol.* **2019**, *37*, 559–565. [CrossRef]
2. Amghizar, I.; Vandewalle, L.A.; Van Geem, K.M.; Marin, G.B. New Trends in Olefin Production. *Engineering* **2017**, *3*, 171–178. [CrossRef]
3. Chang, C. The conversion of methanol and other O-compounds to hydrocarbons over zeolite catalysts. *J. Catal.* **1977**, *47*, 249–259. [CrossRef]
4. Chen, J.Q.; Bozzano, A.; Glover, B.; Fuglerud, T.; Kvisle, S. Recent advancements in ethylene and propylene production using the UOP/Hydro MTO process. *Catal. Today* **2005**, *106*, 103–107. [CrossRef]
5. Tian, P.; Wei, Y.X.; Ye, M.; Liu, Z.M. Methanol to Olefins (MTO): From Fundamentals to Commercialization. *ACS Catal.* **2015**, *5*, 1922–1938. [CrossRef]
6. Ye, M.; Tian, P.; Liu, Z. DMTO: A Sustainable Methanol-to-Olefins Technology. *Engineering* **2021**, *7*, 17–21. [CrossRef]
7. Yarulina, I.; Chowdhury, A.D.; Meirer, F.; Weckhuysen, B.M.; Gascon, J. Recent trends and fundamental insights in the methanol-to-hydrocarbons process. *Nat. Catal.* **2018**, *1*, 398–411. [CrossRef]

8. Mihail, R.; Straja, S.; Maria, G.; Musca, G.; Pop, G. Kinetic model for methanol conversion to olefins. *Ind. Eng. Chem. Process Des. Dev.* **2002**, *22*, 532–538. [CrossRef]

9. Fatourehchi, N.; Sohrabi, M.; Royaee, S.J.; Mirarefin, S.M. Preparation of SAPO-34 catalyst and presentation of a kinetic model for methanol to olefin process (MTO). *Chem. Eng. Res. Des.* **2011**, *89*, 811–816. [CrossRef]

10. Bos, A.N.R.; Tromp, P.J.J.; Akse, H.N. Conversion of Methanol to Lower Olefins-Kinetic Modeling, Reactor Simulation, and Selection. *Ind. Eng. Chem. Res.* **1995**, *34*, 3808–3816. [CrossRef]

11. Ying, L.; Yuan, X.S.; Ye, M.; Cheng, Y.W.; Li, X.; Liu, Z.M. A seven lumped kinetic model for industrial catalyst in DMTO process. *Chem. Eng. Res. Des.* **2015**, *100*, 179–191. [CrossRef]

12. Cui, C.T.; Yin, H.; Yang, J.; Wei, D.M.; Sun, J.S.; Guo, C.N. Selecting suitable energy-saving distillation schemes: Making quick decisions. *Chem. Eng. Process.-Process Intensif.* **2016**, *107*, 138–150. [CrossRef]

13. Ye, H.T.; Zou, X.; Zhu, W.X.; Yang, Y.; Dong, H.G.; Bi, M.S. Synthesis framework for distillation sequence with sidestream columns: Application in reaction-separation-recycle system. *Chem. Eng. Res. Des.* **2021**, *166*, 172–190. [CrossRef]

14. Cui, C.T.; Liu, S.Y.; Sun, J.S. Optimal selection of operating pressure for distillation columns. *Chem. Eng. Res. Des.* **2018**, *137*, 291–307. [CrossRef]

15. Gómez-Castro, F.I.; Rico-Ramírez, V.; Segovia-Hernández, J.G.; Hernández-Castro, S.; González-Alatorre, G.; El-Halwagi, M.M. Simplified Methodology for the Design and Optimization of Thermally Coupled Reactive Distillation Systems. *Ind. Eng. Chem. Res.* **2012**, *51*, 11717–11730. [CrossRef]

16. Fidkowski, Z.T.; Doherty, M.F.; Malone, M.F. Feasibility of Separations for Distillation of Nonideal Ternary Mixtures. *AIChE J.* **1993**, *39*, 1303–1321. [CrossRef]

17. Lucia, A.; Amale, A.; Taylor, R. Distillation pinch points and more. *Comput. Chem. Eng.* **2008**, *32*, 1342–1364. [CrossRef]

18. Ramapriya, G.M.; Selvarajah, A.; Cucaita, L.E.J.; Huff, J.; Tawarmalani, M.; Agrawal, R. Short-Cut Methods versus Rigorous Methods for Performance-Evaluation of Distillation Configurations. *Ind. Eng. Chem. Res.* **2018**, *57*, 7726–7731. [CrossRef]

19. Kraemer, K.; Kossack, S.; Marquardt, W. Efficient Optimization-Based Design of Distillation Processes for Homogeneous Azeotropic Mixtures. *Ind. Eng. Chem. Res.* **2009**, *48*, 6749–6764. [CrossRef]

20. Chen, Y.; Eslick, J.C.; Grossmann, I.E.; Miller, D.C. Simultaneous process optimization and heat integration based on rigorous process simulations. *Comput. Chem. Eng.* **2015**, *81*, 180–199. [CrossRef]

21. Viswanathan, J.; Grossmann, I.E. A Combined Penalty-Function and Outer-Approximation Method for Minlp Optimization. *Comput. Chem. Eng.* **1990**, *14*, 769–782. [CrossRef]

22. Dowling, A.W.; Biegler, L.T. A framework for efficient large scale equation-oriented flowsheet optimization. *Comput. Chem. Eng.* **2015**, *72*, 3–20. [CrossRef]

23. Seidel, T.; Hoffmann, A.; Bortz, M.; Scherrer, A.; Burger, J.; Asprion, N.; Küfer, K.-H.; Hasse, H. A novel approach for infeasible path optimization of distillation-based flowsheets. *Chem. Eng. Sci. X* **2020**, *7*, 100063. [CrossRef]

24. Yu, B.Y.; Chien, I.L. Design and Optimization of the Methanol-to-Olefin Process—Part I: Steady-State Design and Optimization. *Chem. Eng. Technol.* **2016**, *39*, 2293–2303. [CrossRef]

25. Yu, B.Y.; Chien, I.L. Design and Optimization of the Methanol-to-Olefin Process—Part II: Comparison of Different Methods for Propylene/Propane Separation. *Chem. Eng. Technol.* **2016**, *39*, 2304–2311. [CrossRef]

26. Dimian, A.C.; Bildea, C.S. Energy efficient methanol-to-olefins process. *Chem. Eng. Res. Des.* **2018**, *131*, 41–54. [CrossRef]

27. Chen, Y.H.; Hsieh, W.; Chang, H.; Ho, C.D. Design and economic analysis of industrial-scale methanol-to-olefins plants. *J. Taiwan Inst. Chem. Eng.* **2022**, *130*, 103893. [CrossRef]

28. Yin, C.; Sun, H.; Lv, D.; Liu, G. Integrated design and optimization of reactor-distillation sequence-recycle-heat exchanger network. *Energy* **2022**, *238*, 121796. [CrossRef]

29. Hentschel, B.; Peschel, A.; Freund, H.; Sundmacher, K. Simultaneous design of the optimal reaction and process concept for multiphase systems. *Chem. Eng. Sci.* **2014**, *115*, 69–87. [CrossRef]

30. Kong, L.X.; Sen, S.M.; Henao, C.A.; Dumesic, J.A.; Maravelias, C.T. A superstructure-based framework for simultaneous process synthesis, heat integration, and utility plant design. *Comput. Chem. Eng.* **2016**, *91*, 68–84. [CrossRef]

31. Ryu, J.; Kong, L.X.; de Lima, A.E.P.; Maravelias, C.T. A generalized superstructure-based framework for process synthesis. *Comput. Chem. Eng.* **2020**, *133*, 106653. [CrossRef]

32. Trespalacios, F.; Grossmann, I.E. Review of Mixed-Integer Nonlinear and Generalized Disjunctive Programming Methods. *Chem. Ing. Tech.* **2014**, *86*, 991–1012. [CrossRef]

33. Su, Y.; Jin, S.M.; Zhang, X.P.; Shen, W.F.; Eden, M.R.; Ren, J.Z. Stakeholder-oriented multi-objective process optimization based on an improved genetic algorithm. *Comput. Chem. Eng.* **2020**, *132*, 106618. [CrossRef]

34. Yang, X.L.; Ward, J.D. Extractive Distillation Optimization Using Simulated Annealing and a Process Simulation Automation Server. *Ind. Eng. Chem. Res.* **2018**, *57*, 11050–11060. [CrossRef]

35. Qian, X.; Jia, S.K.; Huang, K.J.; Chen, H.S.; Yuan, Y.; Zhang, L. Optimal design of Kaibel dividing wall columns based on improved particle swarm optimization methods. *J. Clean. Prod.* **2020**, *273*, 123041. [CrossRef]

36. Frenkel, M.; Kabo, G.J.; Marsh, K.N.; Beganov, G.N.; Wilboit, R.C. *Thermodynamics of Organic Component in the Gas State*; TRC: College Station, TX, USA, 1994.

37. Smith, R.; Jobson, M. *Distillation*; Academic Press: Oxford, UK, 2000; pp. 84–103. [CrossRef]
38. Luyben, W.L. *Principles and Case Studies of Simultaneous Design*; John Wiley & Sons: Hoboken, NJ, USA, 2011.